Toroidal moments as indicator for magneto-electric coupling: the case of $BiFeO_3$ versus $FeTiO_3$

Claude Ederer
*School of Physics, Trinity College, Dublin 2, Ireland**
(Dated: January 19, 2009)

In this paper we present an analysis of the magnetic toroidal moment and its relation to the various structural modes in *R*3*c*-distorted perovskites with magnetic cations on either the perovskite *A* or *B* site. We evaluate the toroidal moment in the limit of localized magnetic moments and show that the full magnetic symmetry can be taken into account by considering small induced magnetic moments on the oxygen sites. Our results give a transparent picture of the possible coupling between magnetization, electric polarization, and toroidal moment, thereby highlighting the different roles played by the various structural distortions in multiferroic $BiFeO_3$ and in the recently discussed isostructural material $FeTiO_3$, which has been predicted to exhibit electric field-induced magnetization switching.

arXiv:0901.2812v1 [cond-mat.mtrl-sci] 19 Jan 2009

The concept of magnetic toroidal moments in solids has recently received increased attention due to its potential relevance in the context of multiferroic materials and magneto-electric coupling.[1,2,3,4,5] A magnetic toroidal moment represents a vector-like electromagnetic multipole moment which breaks both space and time reversal symmetries simultaneously. It can be represented by a current flowing through a solenoid bent into a torus, or alternatively, by a ring-like arrangement of magnetic dipoles.[6] The toroidal moment has been proposed as the primary order parameter for the low-temperature phase transition from a ferroelectric into a simultaneously ferroelectric and weakly ferromagnetic, i.e. multiferroic, phase in boracites.[7] In addition, the observation of toroidal domains in $LiCoPO_4$ has recently been reported.[2] This suggests that ferrotoroidicity is a fundamental form of ferroic order, equivalent to ferromagnetism, ferroelectricity, and ferroelasticity.[8]

The practical relevance of ferrotoroidic order stems from the fact that the presence of a magnetic toroidal moment also leads to the appearance of an antisymmetric magneto-electric effect.[7,9] This is particularly interesting considering the extensive current research efforts aimed at finding novel multiferroic materials which exhibit strong coupling between magnetization and electric polarization.[10,11,12,13] As suggested in Ref. 3, the toroidal moment concept can offer useful guidance in order to identify possible new candidate systems and to analyze the specific nature of the magneto-electric coupling. At the moment, however, it is not fully clear how this has to be done in practice. It is therefore the purpose of this work to present an instructive analysis of the toroidal moment for an important class of multiferroics, and to illustrate how such an analysis can provide insights into possible coupling between the various order parameters. Specifically, here we evaluate the toroidal moment for the case of the *R*3*c*-distorted perovskite $BiFeO_3$ and the recently proposed isostructural system $FeTiO_3$ (see Ref. 14).

$BiFeO_3$ is probably the most studied multiferroic to date, whereas *R*3*c* $FeTiO_3$ has only recently been proposed as a material that exhibits ferroelectrically-induced weak ferromagnetism, and thus offers the possibility of electric-field controlled magnetization switching.[14,15] First principles calculations show weak ferromagnetism for both $BiFeO_3$ and *R*3*c* $FeTiO_3$.[14,16] The net magnetization in these systems is due to a slight canting of the mainly antiferromagnetically ordered Fe spins. This canting is induced by the Dzyaloshinskii-Moriya interaction.[17,18] A small magnetization has indeed been observed experimentally in thin film samples of $BiFeO_3$,[19,20] whereas in bulk $BiFeO_3$ this effect is canceled out by the presence of an additional cycloidal rotation of the antiferromagnetic order parameter.[21] As was shown by both symmetry analysis and explicit first principles calculations, the weak magnetization is linearly coupled to the spontaneous electric polarization in $FeTiO_3$, but not in $BiFeO_3$.[14,15,16] The analysis of the toroidal moment presented in the following confirms this fact while in addition providing a complementary perspective.

The toroidal moment $\vec{t}$ of a system of localized magnetic moments $\vec{m}_i$ at sites $\vec{r}_i$ can be written as:[4,5,6]

$$\vec{t} = \frac{1}{2}\sum_i \vec{r}_i \times \vec{m}_i \quad . \tag{1}$$

As described in Ref. 4, the presence of the position vector in Eq. (1) together with the periodic boundary conditions encountered in bulk systems lead to a multivaluedness of the toroidal moment, in close analogy to the case of the electric polarization.[22,23] As a result only differences in the toroidal moment (induced for example by a structural distortion) are well defined quantities, and the multivaluedness has to be taken into account when evaluating such toroidal moment differences. A toroidal state is represented by a *spontaneous toroidal moment* $\vec{t}_s \neq 0$, where $\vec{t}_s$ is evaluated as the change in toroidal moment with respect to a non-toroidal reference configuration. On the other hand, a non-toroidal state corresponds to a "centrosymmetric" ensemble of toroidal moment values, but does not necessarily imply that the straightforward evaluation of Eq. (1) for one unit cell leads to $\vec{t} = 0$.[4]

As already discussed in Ref. 4, the toroidal moment of

TABLE I: Coordinates of all ions i within the rhombohedral unit cell of the $R3c$ ABO_3 structure, $\vec{r}_i = a_1\vec{a}_1 + a_2\vec{a}_2 + a_3\vec{a}_3$. Without loss of generality we define the origin to coincide with the position of the first A cation.

i	$A1$	$A2$	$B1$	$B2$	O1	O2	O3	O4	O5	O6
a_1	0	$\frac{1}{2}$	$(\frac{1}{4}+\delta_B)$	$(\frac{3}{4}+\delta_B)$	$(\frac{1}{2}+u)$	w	v	$(\frac{1}{2}+w)$	$(\frac{1}{2}+v)$	u
a_2	0	$\frac{1}{2}$	$(\frac{1}{4}+\delta_B)$	$(\frac{3}{4}+\delta_B)$	v	$(\frac{1}{2}+u)$	w	$(\frac{1}{2}+v)$	u	$(\frac{1}{2}+w)$
a_3	0	$\frac{1}{2}$	$(\frac{1}{4}+\delta_B)$	$(\frac{3}{4}+\delta_B)$	w	v	$(\frac{1}{2}+u)$	u	$(\frac{1}{2}+w)$	$(\frac{1}{2}+v)$

$BiFeO_3$ evaluated in the limit of localized magnetic moments vanishes if one takes into account magnetic moments only on the nominally magnetic Fe sites. This is due to the fact that the antiferromagnetically ordered Fe cation sublattice in $BiFeO_3$ represents a simple rhombohedral lattice, with inversion centers located on each cation site, and thus $\vec{t}_s = 0$. The same holds true for $R3c$ $FeTiO_3$. The symmetry-breaking required for a nonvanishing toroidal moment in these systems is due to the structural distortions exhibited by the oxygen network surrounding the magnetic cations. In the following we will therefore assume that small induced magnetic moments are located on the anion sites in both $BiFeO_3$ and $FeTiO_3$, and we will evaluate the toroidal moment corresponding to these induced magnetic moments on the oxygen sites. Note that if the full magnetization density would be taken into account when evaluating the toroidal moment, then the full magnetic symmetry of the system would automatically be included in the calculation. A formalism for calculating the toroidal moment directly from the quantum mechanical wavefunction has been suggested recently.[24]

In this work, we are considering perovskite-derived systems with structural $R3c$ symmetry,[25] i.e. the crystal structure found experimentally for $BiFeO_3$ at ambient conditions.[26,27] $R3c$ $FeTiO_3$ (and $MnTiO_3$) can be synthesized at high pressure, and remains metastable at ambient conditions, even though the equilibrium crystal structure in this case is the illmenite structure (space group $R\bar{3}$).[28,29]

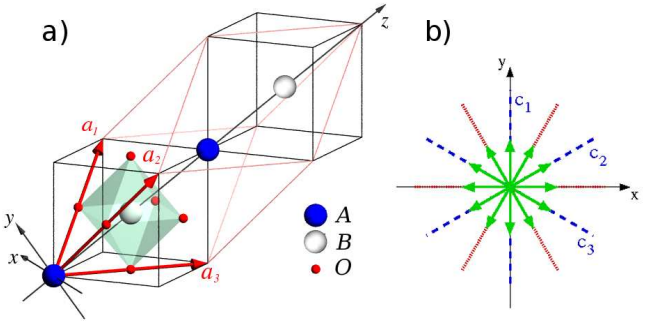

FIG. 1: a) Unit cell definition used in this work. To better visualize the orientation of the coordinate system and rhombohedral basis vectors $\vec{a}_i$, the rhombohedral unit cell is inscribed into two cubes of the underlying perovskite structure. Only ions within one rhombohedral unit cell are shown. The depicted atomic positions correspond to the undistorted case. b) Orientation of the three glide planes $c_{1,2,3}$, and of the 12 equivalent directions for the antiferromagnetic order parameter $\vec{L}$ (arrows) in the x-y plane.

We use a rhombohedral setup with lattice vectors defined as: $\vec{a}_1 = \left(\frac{\sqrt{3}}{2}a, \frac{1}{2}a, \frac{1}{3}c\right)$, $\vec{a}_2 = \left(-\frac{\sqrt{3}}{2}a, \frac{1}{2}a, \frac{1}{3}c\right)$, $\vec{a}_3 = \left(0, -a, \frac{1}{3}c\right)$ (see Fig. 1a). With this choice of coordinate system, the electric polarization is oriented along the z direction, whereas the magnetic order parameters will be oriented within the x-y plane.

The positions of all ions within the unit cell are listed in Table I. The oxygen anions occupy Wyckoff positions $6b$ of the $R3c$ space group. It can easily be seen that $u = v = w = \delta_B = 0$ corresponds to the undistorted "ideal perovskite" case (but in our case with $R\bar{3}m$ symmetry, due to the rhombohedral distortion of the lattice vectors for $c/a \neq 3\sqrt{2}$). In the following it will be convenient to express the oxygen coordinates in a somewhat different form using $u = \delta_O + \frac{2}{3}\epsilon$, $v = \delta_O - \frac{1}{3}\epsilon + \frac{1}{\sqrt{3}}\phi$, and $w = \delta_O - \frac{1}{3}\epsilon - \frac{1}{\sqrt{3}}\phi$. In this notation, the oxygen positions are:

$$\vec{r}_{O1} = \frac{1}{2}\vec{a}_1 + \begin{pmatrix} \frac{\sqrt{3}}{2}a\epsilon - \frac{1}{2}a\phi \\ \frac{1}{2}a\epsilon + \frac{\sqrt{3}}{2}a\phi \\ \delta_O c \end{pmatrix}, \tag{2a}$$

$$\vec{r}_{O2} = \frac{1}{2}\vec{a}_2 + \begin{pmatrix} -\frac{\sqrt{3}}{2}a\epsilon - \frac{1}{2}a\phi \\ \frac{1}{2}a\epsilon - \frac{\sqrt{3}}{2}a\phi \\ \delta_O c \end{pmatrix}, \tag{2b}$$

$$\vec{r}_{O3} = \frac{1}{2}\vec{a}_3 + \begin{pmatrix} a\phi \\ -a\epsilon \\ \delta_O c \end{pmatrix}, \tag{2c}$$

$$\vec{r}_{O4} = \frac{1}{2}(\vec{a}_1 + \vec{a}_2) + \begin{pmatrix} -a\phi \\ -a\epsilon \\ \delta_O c \end{pmatrix}, \tag{2d}$$

$$\vec{r}_{O5} = \frac{1}{2}(\vec{a}_1 + \vec{a}_3) + \begin{pmatrix} -\frac{\sqrt{3}}{2}a\epsilon + \frac{1}{2}a\phi \\ \frac{1}{2}a\epsilon + \frac{\sqrt{3}}{2}a\phi \\ \delta_O c \end{pmatrix}, \tag{2e}$$

$$\vec{r}_{O6} = \frac{1}{2}(\vec{a}_2 + \vec{a}_3) + \begin{pmatrix} \frac{\sqrt{3}}{2}a\epsilon + \frac{1}{2}a\phi \\ \frac{1}{2}a\epsilon - \frac{\sqrt{3}}{2}a\phi \\ \delta_O c \end{pmatrix}. \tag{2f}$$

It can be seen that ϕ, ϵ, and δ_O define three distinct distortions of the oxygen network: δ_O represents the dis-

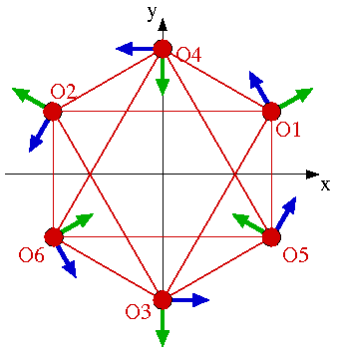

FIG. 2: (Color online) Displacement vectors corresponding to ϕ (blue/dark grey) and ϵ (green/light grey) for the six oxygen anions in the $R3c$ unit cell, viewed along the z direction.

placement of the oxygen anions along the polar axis relative to the A site cations, ϕ represents the counter-rotation of the oxygen octahedra around this axis (including a breathing, i.e. an overall volume change of the octahedra), and ϵ represents an additional deformation of the octahedra, which compresses one side of the octahedron while expanding the opposing side (see Fig. 2).

As stated above, for the completely undistorted structure with $\delta_O = \delta_B = \epsilon = \phi = 0$ the crystallographic symmetry of the system is $R\bar{3}m$. In this case (and if we for now do not consider magnetic order) two primitive cells are included in our unit cell definition. On the other hand, for $\phi \neq 0$ (but otherwise $\epsilon = \delta_O = \delta_B = 0$) the resulting symmetry is $R\bar{3}c$, with doubled primitive cell compared to $\phi = 0$, whereas either $\epsilon \neq 0$, $\delta_O \neq 0$ or $\delta_B \neq 0$ (while all other distortion parameters are zero) leads to polar $R3m$ symmetry (again with two primitive cells contained in our unit cell definition if we neglect magnetic order).

Thus, only $\phi \neq 0$ leads to a crystallographic unit cell doubling compared to the undistorted case (and unrelated to the magnetic order), whereas both δ_O and ϵ break space inversion symmetry and therefore represent polar distortions. In the case of δ_O this is intuitively clear, whereas ϵ is perhaps not immediately recognized as polar. However, ϵ does indeed destroy the inversion symmetry of the system, and it can easily be verified that ϵ also creates an electric polarization $\vec{P} = \sum_i Z_i^* \Delta\vec{r}_i$ if the full Born effective charge tensor (see Ref. 30) is used for Z_i^*. (Here, $\Delta\vec{r}_i$ is the change in the position of oxygen ion i due to $\epsilon \neq 0$.)

It has been correctly pointed out in Ref. 31 that three independent parameters are required to describe the complete distortion of the oxygen network within $R3c$ symmetry. In our notation these three parameters are ϵ, ω, and δ_O. However, in Ref. 31 the distortion ϵ was incorrectly classified as non-polar, which leads to incorrect conclusions about possible magneto-electric coupling in $BiFeO_3$, as will become clear in the following. In fact, as pointed out in Ref. 32, the two displacement patterns represented by ϵ and δ_O (and δ_B as well) correspond to the same irreducible representation Γ_4^- of the original $Pm\bar{3}m$ space group, i.e. they have the same symmetry properties, and can therefore be viewed as two components of the same polar distortion.

We now evaluate the toroidal moment resulting from induced magnetic moments on the oxygen positions listed in Eqs. (2a)-(2f). For this we first have to discuss the symmetry of the magnetically ordered state. First principles calculations suggest that for both $BiFeO_3$ and $R3c$ $FeTiO_3$ the preferred orientation of the Fe magnetic moments, and thus the weak magnetization, is perpendicular to $\vec{P}$.[14,16] This results in 12 energetically equivalent orientations for the antiferromagnetic order parameter $\vec{L} = \vec{m}_{\mathrm{Fe1}} - \vec{m}_{\mathrm{Fe2}}$ within the x-y plane, either parallel or perpendicular to any of the three c-type glide planes of the underlying $R3c$ structure (see Fig. 1b). (Here, $\vec{m}_{\mathrm{Fe1}}$ and $\vec{m}_{\mathrm{Fe2}}$ are the magnetic moments of the two Fe cations within the crystallographic unit cell.) The magnetic order thus breaks the threefold symmetry around the polar z axis and reduces the crystallographic $R3c$ symmetry to the magnetic symmetry groups Cc or Cc', depending on whether the Fe magnetic moments are parallel or perpendicular to the remaining c-type glide plane. (Here, C indicates a base-centered monoclinic Bravais lattice and c' a glide plane combined with time reversal.) In the following we will consider the two representative cases with $\vec{L}$ aligned either along the x direction (Cc' symmetry) or along the y direction (Cc symmetry).

If the antiferromagnetic order parameter defined by the Fe magnetic moments is directed along the x direction, i.e. the magnetic symmetry is Cc', then the y-z plane is a c-type glide plane combined with time reversal. This symmetry operation poses the following restrictions on the magnetic moments $\vec{m}_i$ $(i = 1, \ldots, 6)$ at the oxygen sites: $m_{6x} = -m_{2x}$, $m_{6y/z} = m_{2y/z}$, $m_{5x} = -m_{1x}$, $m_{5y/z} = m_{1y/z}$, $m_{4x} = -m_{3x}$, $m_{4y/z} = m_{3y/z}$. Evaluating Eq. (1) using these relations together with the oxygen positions (2a)-(2f), and considering the multivaluedness according to Ref. 4, results in the following x component of the spontaneous toroidal moment:

$$t_{s,x}^{(Cc')} = \frac{a}{2}\left\{\sqrt{3}\phi\,(m_{1z} - m_{2z}) + 3\epsilon\,(m_{1z} + m_{2z})\right\} \quad . \tag{3}$$

Here, we have imposed the additional constraint that $m_{3z} = -m_{1z} - m_{2z}$, to ensure that $\sum_i m_{iz} = 0$. This corresponds to a decomposition of the full moment configuration into compensated and uncompensated parts to ensure independence of the calculated toroidal moment from the choice of origin (see Ref. 4). We note that both t_y and t_z are vanishing if appropriate multiples of lattice vectors are added to the atomic positions of the oxygen anions. This means that the components of the spontaneous toroidal moment along these directions are zero (see Ref. 4).

The corresponding expression for Cc symmetry, i.e. for orientation of the antiferromagnetic vector $\vec{L}$ along the y

direction, is:

$$t_{s,y}^{(Cc)} = \frac{a}{2}\left\{\phi\left(m_{1z}+m_{2z}-2m_{3z}\right)-\sqrt{3}\epsilon\left(m_{1z}-m_{2z}\right)\right\} \quad . \tag{4}$$

In this case the symmetry restrictions for the oxygen magnetic moments are: $m_{6x} = m_{2x}$, $m_{6y/z} = -m_{2y/z}$, $m_{5x} = m_{1x}$, $m_{5y/z} = -m_{1y/z}$, $m_{4x} = m_{3x}$, $m_{4y/z} = -m_{3y/z}$, and there is also a nontrivial z component of the toroidal moment. However, since this component of the toroidal moment does not contribute to the coupling between $\vec{P}$ and $\vec{M}$ (see below), we only consider t_y.

It can be seen that in general the toroidal moment in $R3c$ $BiFeO_3$ and $FeTiO_3$ is nonzero for both possible magnetic symmetries, and that it is related to the structural distortions of the oxygen network ($\vec{t}_s = 0$ for $\epsilon = \phi = 0$). However, the full functional dependence of $\vec{t}_s$ on ϕ, ϵ, and δ_O can not be seen from Eqs. (3) and (4), since in general the values of the oxygen magnetic moments will also depend on these structural parameters (including also δ_B). To gain further insight into possible magneto-electric coupling we now consider the case $\epsilon = 0$, $\phi \neq 0$, i.e. the paraelectric reference phase with crystallographic $R\bar{3}c$ symmetry. As has been pointed out in Refs. 33, 14, and 15, the presence of a linear magneto-electric effect in the paraelectric reference phase will lead to a linear coupling between the *spontaneous* order parameters $\vec{M}_s$ and $\vec{P}_s$. In contrast, a linear magneto-electric effect in the multiferroic phase describes the coupling of an additional *induced* component of polarization or magnetization to the corresponding reciprocal fields (e.g. $\vec{M}(\vec{E}) = \vec{M}_s + \alpha\vec{E}$). It is therefore very important to clearly distinguish between the presence of a linear magneto-electric effect in the para-phase (where $\vec{M}_s = \vec{P}_s = 0$) and in the multiferroic phase ($\vec{M}_s \neq 0$ and $\vec{P}_s \neq 0$).

We first consider the case $\vec{L} \parallel x$. For $BiFeO_3$ this results in magnetic $C2'/c'$ symmetry, which leads to the additional constraint $m_{2z} = m_{1z}$ and thus vanishing toroidal moment $t_{s,x}^{(C2'/c')} = 0$. For $FeTiO_3$ the resulting symmetry is $C2/c'$, which requires $m_{2z} = -m_{1z}$ and thus $t_{s,x}^{(C2/c')} = \sqrt{3}a\phi m_{1z}$. The difference between $BiFeO_3$ and $FeTiO_3$ in this case results from the different site symmetries of the magnetic Fe sites within $R\bar{3}c$ symmetry. In $R\bar{3}c$ $BiFeO_3$ the Fe cation is located on a site with inversion symmetry, whereas in $R\bar{3}c$ $FeTiO_3$ the inversion centers are located in between the magnetic cations (see also Ref. 15). For the case $\vec{L} \parallel y$ the resulting symmetry is $C2/c$ ($BiFeO_3$) or $C2'/c$ ($FeTiO_3$). The additional constraints on the oxygen magnetic moments are $m_{2z} = -m_{1z}$ and $m_{3z} = 0$ for $C2/c$ symmetry and $m_{1z} = m_{2z}$ for $C2'/c$ symmetry, leading to toroidal moment components $t_{s,y}^{(C2/c)} = 0$ and $t_{s,y}^{(C2'/c)} = a\phi(m_{1z} - m_{3z})$, respectively. The calculated spontaneous toroidal moments for the various cases are summarized in Table II.

It can be seen that in the paraelectric $R\bar{3}c$ phase (i.e. for $\epsilon = 0$) only $FeTiO_3$, but not $BiFeO_3$, has a nonvanishing toroidal moment, and that the toroidal moment in paraelectric $FeTiO_3$ is related to the counter-rotations of the oxygen octahedra represented by ϕ. The presence of this toroidal moment causes a linear magneto-electric effect $\vec{M} = \alpha\vec{E}$ with $\alpha \propto \vec{t}$ via the free-energy invariant $E_{TPM} \propto \vec{t}\cdot\left(\vec{P}\times\vec{M}\right)$ (see e.g. Ref. 4). This means that once the polarization in $R\bar{3}c$ $FeTiO_3$ becomes nonzero (which of course reduces the crystallographic symmetry to $R3c$), it will induce a weak magnetization via the linear magneto-electric effect, consistent with the design criteria outlined in Ref. 14. Such "ferroelectrically-induced ferromagnetism" via the linear magneto-electric effect has been originally suggested in Ref. 33.

TABLE II: Calculated values of the spontaneous toroidal moment and corresponding magnetic symmetry groups for $BiFeO_3$ and $FeTiO_3$ in the paraelectric $R\bar{3}c$ structure ($\epsilon = 0$) for different orientation of the antiferromagnetic order parameter.

	$BiFeO_3$		$FeTiO_3$	
$\vec{L} \parallel \hat{x}$	$C2'/c'$	$\vec{t}_s = 0$	$C2/c'$	$t_{s,x} = \sqrt{3}a\phi m_{1z}$
$\vec{L} \parallel \hat{y}$	$C2/c$	$\vec{t}_s = 0$	$C2'/c$	$t_{s,y} = a\phi(m_{1z} - m_{3z})$

On the other hand, paraelectric $R\bar{3}c$ $BiFeO_3$ is non-toroidal and does not exhibit a linear magneto-electric effect. Therefore, the weak magnetization in $BiFeO_3$ is not ferroelectrically-induced and there is no linear coupling between $\vec{M}_s$ and $\vec{P}_s$ in the multiferroic phase. This is also consistent with first principles calculations, where for $BiFeO_3$ weak ferromagnetism occurs in both the ferroelectric $R3c$ and the paraelectric $R\bar{3}c$ structures, whereas for $FeTiO_3$ it occurs only in the ferroelectric $R3c$ structure.[14,16]

Note that in the multiferroic $R3c$ phase both $FeTiO_3$ and $BiFeO_3$ exhibit a toroidal moment (according to Eqs. (3) and (4)) and thus a linear magneto-electric effect. This means that an external electric field will induce changes in both polarization and magnetization, linear in the external field, but only in $FeTiO_3$ the corresponding spontaneous order parameters $\vec{M}_s$ and $\vec{P}_s$ are linearly coupled. Such linear coupling between $\vec{P}_s$ and $\vec{M}_s$ is required to achieve full electric-field control of the weak magnetization. As outlined in Refs. 14 and 15 a reversal of $\vec{P}_s$ in $FeTiO_3$ induced by an external electric field will result in a corresponding reversal of $\vec{M}_s$ provided the antiferromagnetic order parameter (or equivalently the toroidal moment) is fixed by a large enough magnetic anisotropy. On the other hand, such electric field controlled switching of the weak magnetization is not expected to occur in $BiFeO_3$.

The evaluation of the toroidal moment presented above allows to clearly identify which structural modes, in combination with the antiferromagnetic order, lead to the appearance of a toroidal moment and a linear magneto-electric effect. In contrast to the antiferromagnetic order parameter, which generally depends only on the orienta-

tion of the individual magnetic moments, it follows from Eq. (1) that the toroidal moment contains information about where the magnetic moments are located as well as on how they are oriented. Furthermore, the toroidal moment is a macroscopic multipole moment that is related to the (magnetic) point group symmetry, whereas a proper symmetry analysis of antiferromagnetic order requires a treatment based on the full space group symmetry. In particular, antiferromagnetic order is not connected to any particular macroscopic symmetry breaking, i.e. all 90 magnetic point groups are compatible with the existence of antiferromagnetic order. On a microscopic space group level, antiferromagnetic order of course always breaks time reversal symmetry. However, for systems where the magnetic unit cell is a multiple of the crystallographic unit cell, a primitive translation of the original nonmagnetic lattice can be combined with time reversal, and as a result the corresponding magnetic point group still contains time reversal as a symmetry element.[34] In contrast, a toroidal moment always breaks space and time reversal symmetries on the macroscopic level, i.e. the corresponding magnetic point group does not contain neither space inversion $\bar{1}$ nor time reversal $1'$ (whereas the combined operation $\bar{1}'$ can still be a symmetry element). Since all macroscopic properties of a particular crystal are determined by its point group rather than space group symmetry,[34] the toroidal moment appears to be a more appropriate quantity to classify macroscopic symmetry properties compared to the antiferromagnetic order parameter. In particular, the toroidal moment is ideally suited to discuss magneto-structural or magneto-electric coupling. For a given structural and magnetic configuration the toroidal moment can be evaluated straightforwardly, applying the procedure outlined in Ref. 4. Using the relation between the toroidal moment and the magneto-electric tensor α, this allows to correctly identify which quantities determine the magneto-electric properties of the system. The same can of course also be achieved by a group theoretical analysis of the symmetry properties of the various structural modes and of the antiferromagnetic order parameter. The straightforward evaluation of the toroidal moment should therefore be considered as an alternative (or complementary) way to discuss magneto-electric symmetry that does not necessarily require the application of group theoretical concepts.

Finally, we point out that the toroidal moment is only related to the antisymmetric part of the linear magneto-electric tensor α, whereas the symmetric part of α is connected to other electromagnetic multipole moments (see Ref. 5). However, for the present case where weak ferromagnetism is caused by the Dzyaloshinskii-Moriya interaction, the antisymmetric component related to the toroidal moment is indeed the crucial part of α.

In summary, we have shown that by evaluating the toroidal moment in the limit of localized magnetic moments, a clear picture of the different roles played by the various structural distortions for the magneto-electric properties in $BiFeO_3$ and $R3c$ $FeTiO_3$ can be achieved. The toroidal moment can be used to characterize the magneto-electric properties in antiferromagnetic systems. Its usefulness stems from the fact that is depends on both position and orientation of the magnetic moments and from its well-defined macroscopic symmetry properties, which allow to use point groups instead of space groups, in contrast to a discussion based on the antiferromagnetic order parameter.

Acknowledgments

This work was supported by Science Foundation Ireland under Ref. SFI-07/YI2/I1051.

* Electronic address: edererc@tcd.ie

1 H. Schmid, in *Magnetoelectric interaction phenomena in crystals*, edited by M. Fiebig, V. Eremenko, and I. E. Chupis (Kluwer, Dordrecht, 2004), pp. 1–34.

2 B. B. Van Aken, J. P. Rivera, H. Schmid, and M. Fiebig, Nature **449**, 702 (2007).

3 K. M. Rabe, Nature **449**, 674 (2007).

4 C. Ederer and N. A. Spaldin, Phys. Rev. B **76**, 214404 (2007).

5 N. A. Spaldin, M. Fiebig, and M. Mostovoy, J. Phys.: Condens. Matter **20**, 434203 (2008).

6 V. M. Dubovik and V. V. Tugushev, Physics Reports **4**, 145 (1990).

7 D. G. Sannikov, J. Exp. Theo. Phys. **84**, 293 (1997).

8 H. Schmid, Ferroelectrics **252**, 41 (2001).

9 A. A. Gorbatsevich, Y. V. Kopaev, and V. V. Tugushev, Sov. Phys. JETP **58**, 643 (1983).

10 N. A. Spaldin and M. Fiebig, Science **309**, 391 (2005).

11 W. Eerenstein, N. D. Mathur, and J. F. Scott, Nature **442**, 759 (2006).

12 S.-W. Cheong and M. Mostovoy, Nature Materials **6**, 13 (2007).

13 R. Ramesh and N. A. Spaldin, Nature Materials **6**, 21 (2007).

14 C. J. Fennie, Phys. Rev. Lett. **100**, 167203 (2008).

15 C. Ederer and C. J. Fennie, J. Phys.: Condens. Matter **20**, 434219 (2008).

16 C. Ederer and N. A. Spaldin, Phys. Rev. B **71**, 060401(R) (2005).

17 I. E. Dzyaloshinskii, Sov. Phys. JETP **5**, 1259 (1957).

18 T. Moriya, Phys. Rev. **120**, 91 (1960).

19 W. Eerenstein, F. D. Morrison, J. Dho, M. G. Blamire, J. F. Scott, and N. Mathur, Science **307**, 1203a (2005).

20 H. Bea, M. Bibes, S. Petit, J. Kreisel, and A. Barthelemy, Philos. Mag. Lett. **87**, 165 (2007).

21 I. Sosnowska, T. Peterlin-Neumaier, and E. Streichele, J. Phys. C **15**, 4835 (1982).

22 R. D. King-Smith and D. Vanderbilt, Phys. Rev. B **47**,

R1651 (1993).
[23] R. Resta, Rev. Mod. Phys. **66**, 899 (1994).
[24] C. D. Batista, G. Ortiz, and A. A. Aligia, Phys. Rev. Lett. **101**, 077203 (2008).
[25] Depending on the amount of distortion, the corresponding structure is sometimes referred to as the "ferroelectric $LiNbO_3$ structure". This distinction between distorted perovskite and $LiNbO_3$ structure is purely quantitative and thus not relevant in the present context.
[26] C. Michel, J.-M. Moreau, G. D. Achenbach, R. Gerson, and W. J. James, Solid State Commun. **7**, 701 (1969).
[27] F. Kubel and H. Schmid, Acta Crystallogr. Sect. B **46**, 698 (1990).
[28] J. Ko and C. T. Prewitt, Phys. Chem. Miner. **15**, 355 (1988).
[29] L. C. Ming, Y.-H. Kim, Y. Uchida, Y. Wang, and M. Rivers, Am. Mineral. **91**, 120 (2006).
[30] P. Ghosez, J.-P. Michenaud, and X. Gonze, Phys. Rev. B **58**, 6224 (1998).
[31] R. de Souza and J. E. Moore, arXiv:0806.2142 (2008).
[32] C. J. Fennie, arXiv:0807.0472 (2008).
[33] D. L. Fox and J. F. Scott, J. Phys C **10**, L329 (1977).
[34] R. R. Birss, *Symmetry and Magnetism* (North Holland Pub., Amsterdam, 1966).